研究論文

초음파시험에 의한 용접결함의 종류판별과 크기산정의 새로운 기법

송 성 진*

New Approaches to Ultrasonic Classification and Sizing of Flaws in Weldments

S. J. Song*

Key Words : Flaws in Weldments(용접결함), Flaw Classification(결함분류), Neural Networks(신경회로망), Flaw Sizing(결함 크기산정), Time-of-Flight Equivalent Flaw Sizing(비행시간 등가결함 크기산정)

Abstract

Flaw classification(determination of the flaw type) and flaw sizing(prediction of the flaw shape, orientation and sizing parameters) are very important issues in ultrasonic nondestructive evaluation of weldments. In this work, new techniques for both classification and sizing of flaws in weldments are described together with extensive review of previous works on both topics. In the area of flaw classification, a methodology is developed which can solve classification problems using probabilistic neural networks, and in the area of flaw sizing, a time-of-flight equivalent(TOFE) sizing method is presented.

1. INTRODUCTION

All kinds of engineering materials and structures, especially weldments, have flaws, some of which can cause catastropic failures. In modern high performance engineering applications, the structural integrity of these materials and structures are quite often evaluated using fracture mechanics. This evaluation in turn requires information on the flaw geometry (location, type, shape, size, and orientation). The ultrasonic nondestructive evaluation(NDE) method is one technique that is commonly used to provide such information. Usually, the ultrasonic flaw characterization process involves two steps : flaw classification(determination of the flaw type) and flaw sizing(prediction of the flaw shape, orientation and size parameters). In this paper new approaches to both classification and sizing of flaws in weldments are described together with extensive

review of previous works on both topics. The techniques proposed here are in a form that can be used directly in many practical applications to quantitative estimates of the flaw's significance.

2. ULTRASONIC FLAW CLASSIFICATION

Cracks are usually considered more dangerous than non-crack-like(volumetric) defects. Thus, it is common to try to classify only between more severe (crack-like) and less severe(volumetric) flaws. For weldments, however, it is desirable to introduce more flaw classification categories(such as cracks, porosity and slag inclusions) not only for the evaluation of the structural integrity of the weld but also for the improvement of the weld process performance.

In conventional ultrasonic NDE, flaw classification is usually done by a human operator based on heuristic experience-based echodynamic pattern identification techniques[1, 2]. Unfortunately, these methods are highly operator dependent and often do not perform well in practice.

Recently, there have been developed model-based quantitative classification techniques which extensively use amplitude information of the ultrasonic signals received from flaws. Shcherbinskii and Belyi[3], for example, proposed the use of "form factors" of flaws which are features that can be measured with a tandem transducer method. Expanding this concept, Volpinkin[4] developed a modified method which can be applied to classifying flaws in weldment. The satellite-pulse technique developed by Gruber[5] also falls into this category. Very recently, Chiou and Schmerr[6] developed a new scheme which can distinguish smooth vs. sharp-edged flaws by use of the time-separation and amplitude difference of mode-converted diffracted signals in a quasi-pulse-echo configuration. On the other hand, there has been work on the use of features extracted from the frequency domain of ultrasonic signals. This approach is known as ultrasonic spectral analysis[7, 8] and typically uses broadband ultrasonic pulses. Fitting and Adler[9] have reviewed previous work in this area in detail.

All of the methods mentioned above need to capture very "strong" features so that the flaw type information can then be directly decided by a human operator. Unfortunately, in many realistic situation the classification problems are not so simple and the criteria fuzzy. To take care of this difficulty, new approaches using "ultrasonic pattern recognition" techniques, have been introduced that use a variety of modern digital signal processing techniques, and various decision-making algorithms. This approach involves three steps : 1) measurement of the ultrasonic signals from flaws, 2) the extraction of a set of features from those measurements which can serve as a basis for a given classification problem, often using digital signal processing techniques, and 3) solving the given classification problem using these features and a specific decision-making criterion.

Some of the earlist work related to ultrasonic pattern recognition was done by Rose and his co-workers[10~12]. They extracted physically based features from the ultrasonic time domain signals and adopted the Fisher linear discriminant function as a classifier. Burch and Bealing[13] used a similar approach to classify relatively large buried flaws in ferritic steel welds into four different groups. In their work, they used more general features extracted from the time domain and a weighted minimum distance pattern recognition algorithm as a classification rule. In a following study, Burch[14] expanded this idea to classification problem of vertical and near vertical planar defects using a combination of pulse-echo and tandem techniques.

The rapid advance in the field of artificial intelligence(AI) has stimulated the development of some approaches which extensively use AI concepts. For example, Mucciadi and his co-workers[15, 16] developed an ultrasonic inversion procedure which discriminated and sized flaws by the use of adaptive learning networks, using features extracted from the power spectrum. Recently, Koo[17] presented a flaw classification system using modeling, signal processing and adaptive learning networks. In his work, he used more "fundamental"(model-based) features extrac-

ted from the time domain. A rule-based expert system approach has also been used to solve ultrasonic flaw classification problems by Schmerr and his co-workers[18, 19]. In this case, nine "fundamental" features extracted from the time and frequency domains were used. More recently, artificial neural networks have seen applications in this area.

Artificial neural networks[20, 21] loosely model the structure and operation of the human brain. They are composed of richly interconnected simple processing elements which can operate simultaneously to achieve high speed data processing. They have the ability to approximate arbitrary mappings from sets of input-output patterns presentations. Furthermore, once trained, they can produce outputs "instantaneously." The recent discovery of new training algorithms such as back-propagation[22] has brought widespread interest in the application of neural networks to various fields. In the field of NDE, neural networks trained by the back-propagation algorithm have been used to solve a variety of sizing and classification problem[23~26]. However, "back-propagation" neural networks have been criticized because of some important disadvantages. These disadvantages include the need for a trial-and-error based determination of the optimal network structure, lengthy training times, and opaqueness of the way in which neural net reaches its "conclusions." Recently, a probabilistic neural network(PNN)[27~30] model has been developed that has all the advantages of neural networks mentioned above but without the typical disadvantages. In the first topic of this work, we present an ultrasonic flaw classification problem in weldments that can be solved by use of the PNN.

3. ULTRASONIC FLAW SIZING

Obtaining flaw size, shape and orientation information from ultrasonic measurements is one example of having to solve an inverse problem of elastic wave scattering. Conventional ultrasonic NDE techniques have not been particularly effective in solving such problems even though a wide variety of ultrasonic flaw sizing approaches[31~33] have been developed including amplitude-based and time-of-flight methods, detailed imaging methods, and equivalent sizing methods.

Conventional field inspections have used only the amplitude information of ultrasonic signals for flaw sizing. For small flaws they have often simply relied on the comparison of the amplitude of flaw signals with those of standard references, like flat bottom holes, of known size. This method has been known as the use of Distance-Gain-Size(DGS) curves and was first formulated and experimentally determined by Krautkramer[34].

Even though this method has a wide variety of applications[2], very few following studies have considered the DGS approach after Krautkramer's original work. Recently, however, Schmerr and Sedov [35] and Sedov, Schmerr and Song[36] have described new ultrasonic scattering models for the pulse-echo response of a flat-bottom hole in contact and immersion testing, respectively. An important feature of these models is their ability to predict both the near-field and far-field response of a flat-bottom hole, whose axis is aligned with the axis of a piston transducer. These predictions were shown to be in good agreement with experiments when single frequency DGS-like curves were considered[36].

More recently Song, Schmerr and Sedov[37] show that "true" DGS curves(obtained from the time-domain amplitude measurements as in Krautkramer's original approach) can be developed easily from these models through deconvolution procedures and Fourier analysis. These theoretical DGS curves are shown to be in good agreement with experiments even in the very near-field. Finally we also use the models to predict frequency response curves that compare favorably with experimental results in both the near and far-fields.

The use of DGS curves is restricted to flaws smaller than the beam size of a transducer. For sizing relatively large flaws, echodynamic patterns[1, 2] have been extensively used, based on mapping the amplitude variation as a function of position of a transducer scanning over a flaw. These conventional approaches, however, are often not quantitative

enough to produce the size information needed for modern fracture mechanics calculations[38].

Some advanced techniques attempt to avoid limitations of conventional amplitude-only approaches by use of time-of-flight information or a combination of time-of-flight and amplitude information. There are, for example, the Time-of-Flight Diffraction(TOFD) method[39~41] and the Satellite-Pulse techniques[5, 42]. Even though these techniques have achieved successes in some applications, they still have some important limitations in the information they can extract about flaw geometry.

To get more complete information about flaw geometry, various detailed imaging method have been developed[43] including the Synthetic Aperture Focussing Technique(SAFT)[44, 45], and the amplitude and transit time locus curves(ALOK)[46], acoustical holography[47], and ultrasonic tomography[48]. These techniques require detailed scanning and considerable data processing. Even after this time consuming process, the results sometimes cannot be directly used for fracture mechanics calculations.

In between the two extremes of conventional methods and detailed scanning methods, there is a model-based approach called equivalent flaw sizing[49~51]. In this approach, flaws are reconstructed in terms of "best-fit" equivalent ellipsoids(for volumetric flaws) or ellipses(for cracks) obtained from a relatively small number of ultrasonic measurements at different transducer orientations and locations. This approach has been developed based on ultrasonic scattering models such as the Born approximation for volumetric flaws[49, 50] or the Kirchhoff approximation for cracks[51]. Recently, a unified algorithm that can be applied to both volumetric flaws and cracks was developed by Schmerr and et al.[52].

For the successful implementation of this approach, there are two major issues which one has to consider : 1) accuracy of experimental measurement of the equivalent radius, which is defined as the distance from the flaw centroid to the front surface tangent plane, and 2) the efficiency of the optimization algorithm used to determine the best-fit flaw parameters from the measured equivalent

radius data.

The equivalent radius, which is the one of the basic parameters on which most current equivalent flaw sizing methods rely, is normally obtained, for small flaws directly from the ultrasonic waveform itself by use of signal processing. Unfortunately, most current methods to determine this quantity suffer from the so-called "zero-of-time" problem[53, 54, 55]. Even though efforts still continue to be undertaken to solve this problem[56], no entirely satisfactory and general solution is currently available.

The efficiency of the optimization scheme(the second issue mentioned above) in the past was an important issue because of the very complicated nonlinear nature of the problem[50]. Fortunately, Chiou and Schmerr[57] have recently eliminated this issue by developing a new approach where they reformulated the optimization problem into a two-step problem involving a simple linear least squares optimization step and the solution of a straightforward eigenvalue problem. In this study, we take advantage of this two-step algorithm in the development of our new equivalent flaw sizing techniques.

In the second topic of this paper, we show how the equivalent flaw sizing concept can be combined with simple time-of-flight measurements to produce a new time-of-flight equivalent(TOFE) sizing method.

4. NEURAL NETWORK APPROACH TO ULTRASONIC FLAW CLASSIFICATION IN WELDMENTS

Here, we will briefly describe a neural network approach to ultrasonic flaw classification in weldments using probabilistic neural networks. We will describe the structure of probabilistic neural network and illustrate its use in distinguishing cracks, porosity, and slag inclusions in weldments based on an ultrasonic data set provided by Westinghouse Corporation.

4.1 THE PROBABILISTIC NETWORK

The basic architecture of the probabilistic neural network is shown in Fig. 1. The network contains four layers whose structures consist of 1) an input layer, where the features to be used by the network are presented, 2) a set of pattern units where each of these units accepts a weighted sum of the inputs and applies a gaussian activation function to that sum at its output. and 3) a set of third layer units(which are connected to each pattern unit of the appropriate class) that sum the outputs of the attached pattern units, weights that sum by a user-defined "cost factor" and presents the resulting output to the fourth and final output layer.
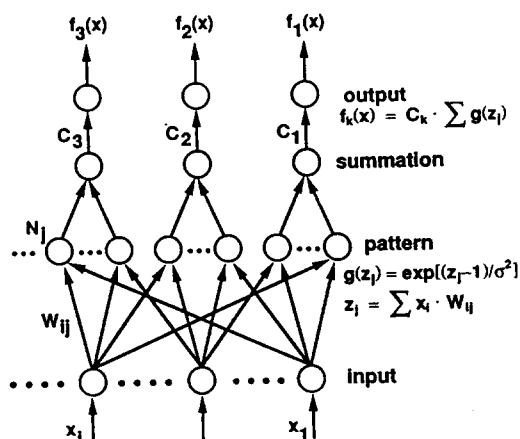

Fig. 1. Probabilistic neural network architecture.

Unlike other neural networks, the probabilistic neural network architecture is strictly determined by the number and choice of training examples (every pattern unit corresponds to a particular training example). The weights, W_{ij}(Fig. 1) are also determined completely by the training set since they are obtained directly from the input features of each training example. In fact, the only adjustable parameters in the network are the cost factors, C_i, and the smoothing constant, σ in the activation functions(Fig. 1), whose determi-

nation will be discussed shortly.

4.2 INPUT FEATURES

The success of any neural network often depends crucially on the choice of the input features. Ideally, these features should be distinguishing characteristics of the different flaw classes and "fundamental" in the sense that they are based on the physics of the scattering process. Since the data set provided to us by Westinghouse was not taken specifically to extract any particular set of such features, we used a variety of more heuristic features as inputs. As shown in Table 1, these features consisted of ten time domain features and four frequency domain features.

Table 1. Input features to the PNN

Time Domain Features
1) number of signal groups
2) pulse duration of the 1st group signal
3) pulse duration of the 2nd group signal
4) pulse duration of the 3rd group signal
5) energy of the 1st group signal
6) energy of the group signal
7) energy of the 3rd group signal
8) interval between the 1st and the 2nd groups
9) interval between the 2nd and the 3rd groups
10) antisymmetry of signal

Frequency Domain Features
11) number of maxima of the magnitude spectrum
12) number of minima of the magnitude spectrum
13) number of deep minima of the magnitude spectrum
14) number of shallow minima of the magnitude spectrum

4.3 NETWORK TRAINING

In the probabilistic neural network, the training method is a very simple three stage process(Fig. 1) :

1. Given the choice of inputs, a second layer output node, N_j($j=1,2 \cdots N$) is chosen for each of the N training examples.

2. If we let X_{ij}($i=1,2 \cdots M$, $j=1,2 \cdots N$) denote

the M features corresponding to each training example, then the weights, W_{ij}, between the jth second layer node and the ith input feature, X_i, are obtained by simply setting $W_{ij} = X_{ij}$.

3. Finally, each second layer pattern unit is connected to the summation unit which corresponds to the class of that training example.

4.4 CHOICE OF NETWORK PARAMETERS

Once the network is trained, as described above, the only remaining parameter choices are the cost factors C_i (i=1,2,3) and the "smoothing" parameter σ(Fig. 1). The cost factors can be simply set equal to one, in which case all output flaw classes(cracks, porosity, slag) are weighted equally. However, if the user wishes to place a stronger weight on a particular class, say cracks, the C_i can be used to adjust the decision-making process. The smoothing parameter, σ, in contrast, is used to adjust the collective importance of each of the individual patterns in the second layer pattern units[27-29]. A small value of σ tends to emphasize the individual patterns while a large value of σ instead smoothes out the behavior over many patterns. The choice of σ is normally made on a trial and error basis with the optimal σ being one which both produces "good" classification results as well as a stable behavior of the network over a wide range of σ-values

4.5 PERFORMANCE OF PNN

The data provided to us by Westinghouse Corp. consisted of 239 digitized ultrasonic waveforms that were taken from contact transducers on mild steel blocks. The blocks had a stainless steel cladding and contained manufactured defects to simulate cracks(104 waveforms), porosity(53 waveforms) and slag(82 waveforms) in weldments. The input features listed in Table 1 were extracted from these waveforms and approximately half of these waveforms were used to train the network. The remaining waveforms served as a testing set to evaluate

the network performance. The two performance evaluation criteria that were used in this study were the correct accept rate, $(CA)_i$ and the false reject rate, $(FR)_i$ for each of the three classes(i=1,2,3) where $(CA)_i$ and $(FR)_i$ are defined as :

$$(CA)_i = \frac{m_i}{n_i} \qquad (i=1, 2, 3) \qquad (1)$$

m_i = number of testing examples from class i classified correctly

n_i = total number of testing examples from class i

$$(FR)_i = \frac{\sum_j m_{ji}}{\sum_j n_i} \qquad j \neq i \qquad (2)$$

m_{ji} = number of testing examples from class j classified as class i

n_i = total number of testing examples from class j

Figures 2a,b show plots of the correct accept rate and of the false reject rate, respectively, for each of the three flaw classes for $C_i = 1$(i=1, 2, 3) and the parameter σ varied over a range of 0−0.3. This range of σ-values we found produced the highest correct accept rates, and, as Figures 2a,b show,
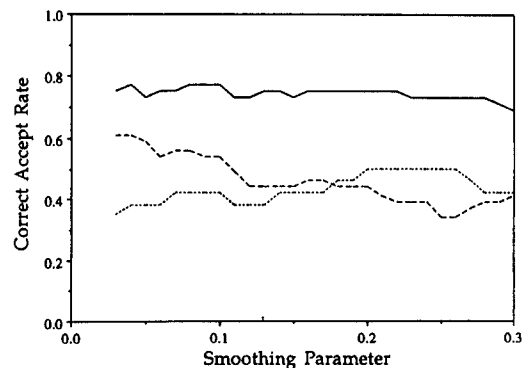

Fig. 2a. Correct accept rates of welding defects by the PNN for different choices of the smoothing parameter σ and with $C_i = 1$ for all. Cases : cracks(solid line), porosity(small dashes), and slag inclusion(large dashes)

Fig. 2b. False reject rates of welding defects by the PNN for different choices of the smoothing parameter σ and with $C_i = 1$ for all Cases : cracks(solid line), porosity(small dashes), and slag inclusion(large dashes)
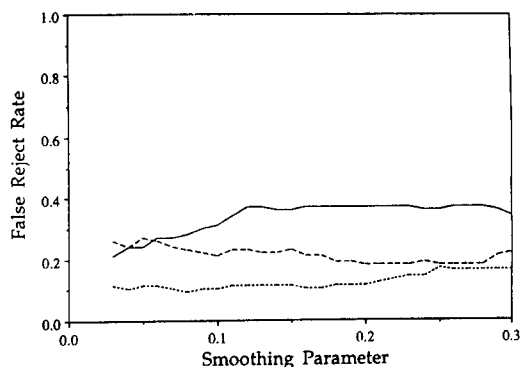

Fig. 3. Influence of the choice of the Ci parameter on PNN performance.

the network performance did not vary substantially with the choice of σ in this range. Although the correct accept rates are lower here than what we would like to see in a production classification system, our extensive experience with this data set suggests that this performance is the best that can be expected for this set of experiments. Since the particular choice of σ was not crucial here, we arbitrarily picked σ = 0.1 for all subsequent testing.

Figures 3a,b,c show the behavior of the network when different cost factors C_i were used for each class. By making the cost factor for cracks higher than those for slag or porosity, the correct accept rate for cracks can be significantly improved but only at the price of increased false rejects for cracks also.

Theoretically, for small σ the PNN should behave similar to a K-nearest neighbor(KNN) classifier, which is a very simple and popular classical classifier [27~29]. Song and Schmerr have shown that there is no practical difference between the performance of the PNN and that of the KNN[30]. However, the PNN does have the advantage over the KNN classifier of being able to complete classifications very rapidly and to produce estimates of the actual probability distributions of the flaw classes at the outputs. Furthermore, It is worthwhile to point out that the
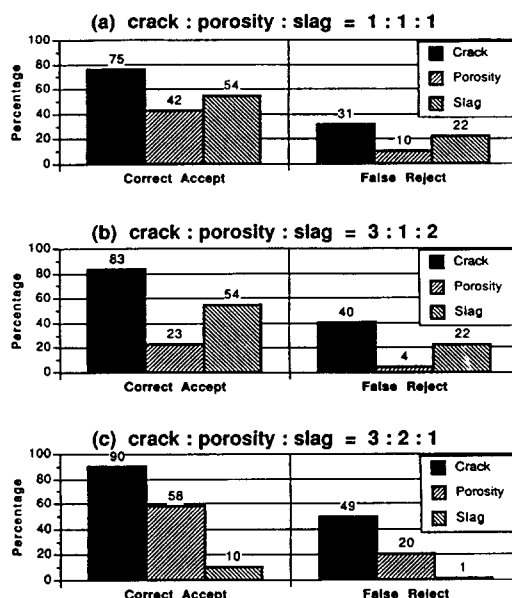
PNN itself has ability to identify good input features for classification[30]. Very recently the author has shown the use of PNNs for robust feature determination[50].

5. TIME-OF-FLIGHT EQUIVALENT FLAW SIZING METHOD

In this section, a new approach to the equivalent flaw sizing, a time-of-flight equivalent(TOFE) sizing method will be described. It will be shown that TOFE sizing is indeed a viable method provided that the flaw is relatively large.

5.1 THE TOFE SIZING ALGORITHM

Figure 4 shows a typical immersion ultrasonic set-up and an "equivalent" flaw, assumed ellipsoidal in shape, whose centroid is located at $\underline{X_c}$. From that figure we see that

$$(X_i^j - X_c) \cdot n_2^j = H_2^j + r_e \tag{3}$$

where X^j_I is the location of the entrance point for the center of the beam of sound into the second material for the jth measurement. The unit vector n^j_2 is parallel to the wave propagation direction in the second medium for the jth measurement and H^j_2 is the distance from the entrance point to the tangent plane of the flaw for the jth measurement. Finally, r^j_e is the equivalent radius of the flaw(distance from the centroid to the tangent plane) for the jth measurement.
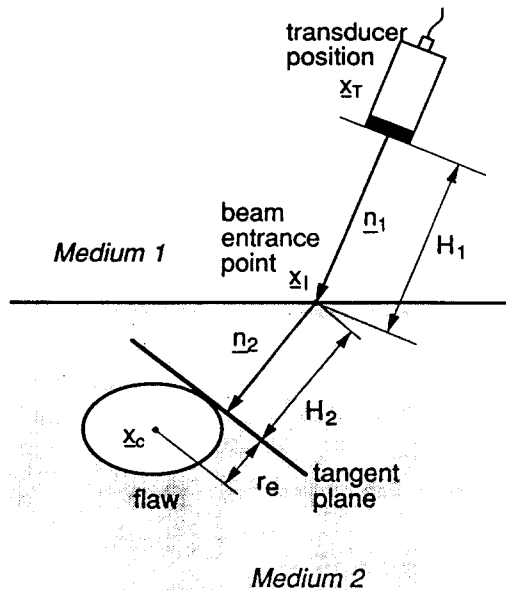

Fig. 4. The measurement geometry of the TOFE sizing method for a flaw embedded in a second medium.

From an A-scan response, a time-of-flight measurement to the interface($\Delta T_1 = 2H_1/C_1$) can be made for each transducer position and orientation and the corresponding time-of-flight to the flaw in the second medium($\Delta T_2 = 2H_2/C_2$) also measured. Then, since the transducer position, X^j_T, and orientation, n^j_1, are both known, X^j_I in eq. (1) can be calculated by

$$X^j_I = X^j_T + H^j_1 \; n^j_1 \tag{4}$$

and n^j_2 can be determined through Snell's law. Thus, all the quantities in eq. (3) are known except the flaw centroid, X_c, and the equivalent radius, r^j_e, at each measurement. However, Chiou and Schmerr[5] have shown that r^j_e can be written in terms of a symmetric matrix C and the unit vector n^j_2 as

$$(r^j_e)^2 = n^j_2 \cdot C n^j_2 \tag{5}$$

Placing equation (5) into equation (3), we can then show that

$$F_j = (X_c \cdot n^j_2)^2 - 2(X_c \cdot n^j_2 - H^j_2)(X_c \cdot n^j_2)$$
$$- n^j_2 \cdot C \; n^j_2 + (X_c \cdot n^j_2 - H^j_2)^2 = 0 \tag{6}$$

where F_j is a linear function of the six matrix elements of C and a quadratic function of the flaw centroid coordinates, X_c. Thus, a non-linear least squares procedure can be used to estimate these nine unknowns by performing N measurements and then minimizing the quantity

$$I(X_c, C) = \sum_{j=1}^{N} [F_j(X_c, C, X^j_I, n^j_2, H^j_2)]^2 \tag{7}$$

Once the C parameters are obtained in this manner, the solution of the eigenvalue problem

$$C - \lambda I = 0 \tag{8}$$

then yields the best-fit ellipsoid and its orientation since, as Chiou and Schmerr[5] have shown, the eigenvalues of C are just the squares of the three principal ellipsoidal axes(a^2, b^2, c^2) and the corresponding eigenvectors are the three unit vectors along these axes. Although minimizing I in eq. (7) is a non-linear optimization problem, since the non-linearity in F_j is at most quadratic in form this optimization problem should not be difficult to solve, a feature of this method that has been verified in practice.

Note that the method also yields an estimate for the flaw centroid location, X_c. Thus, the TOFE sizing method does not require an apriori estimate of this location and hence does not suffer from the zero-of-time problem[4]. However since the TOFE si-

zing method uses time-of-flight measurements to estimate the distance parameters appearing in eqs. (4), (6), it is essential that the wavespeed in all the materials be determined accurately of the TOFE sizing method will produce unacceptably large errors. For example, if there is an error ΔC in the measurement of the wavespeed over a path length H ($H = H_1$ or H_2) then there will be an error in the estimation of the flaw surface location given by

$$\Delta H = (\Delta C / C) H \qquad (9)$$

If the wavespeed were only known to within, say, 2% over a 2 inch(25.4 ㎜) path in steel, ΔH would be approximately 1 ㎜. Because of this fact, we can say that TOFE will typically work only for "relatively large" flaws. The precise meaning of "relatively large", of course, is a function of how accurately the wavespeeds are known and the path length involved in a particular problem.

5.2 INITIAL TESTING WITH SYNTHETIC DATA

For the initial test of the TOFE method, "exact" synthetic data was generated for known flaws immersed in a single medium using 19 simulated time-of-flight measurements over a one-sided scanning aperture angle of 120 degrees. In this case the algorithm simplifies considerably since we can take $x_i' = x_T'$(Fig. 4). Four different flaw shapes were considered : a round ellipsoid, a pancake-like flat ellipsoid, a circular crack, and an elliptical crack, all which have the same location and the same orientation but different sizes. For all flaws the best-fit flaw parameters were determined by the TOFE sizing algorithm using the same set of initial guesses of the flaw centroid location($x_{cx} = 0.0$, $x_{cy} = 0.0$, $x_{cz} = 0.0$) and the C parameters($C_{xx} = 10.0$, $C_{yy} = 10.0$, $C_{zz} = 10.0$, $C_{xy} = 10.0$, $C_{xz} = 10.0$, $C_{yz} = 10.0$). As shown in Table 2, the TOFE method gave the "exact" results (flaw centroid location, size, and orientation) with only 7 − 16 iterations. Using different sets of initial guesses produced the same results with only slight

variations in the number of iterations. Thus, the TOFE sizing method is essentially insensitive to the choice of initial guesses, as expected from the quadratic nonlinearity of Eq. (6).

Table 2. TOFE sizing results for error free synthetic data   (unit : mm)

shape	a	b	c	# of iterations
Ellipsoid				
round	20	25	30	16
pancake	10	5	0.5	9
Crack				
circular	10	10	0	7
elliptical	10	5	0	8

As mentioned previously, one of the important parameters in equivalent sizing using the TOFE sizing scheme is the ultrasonic velocity in the material, since this is an essential factor for converting the time-of-flight from the transducer to the tangent plane to the corresponding distance, H. Thus the wave velocity in the material should be known a priori for application of the TOFE sizing method. This information is usually available from other independent experiments.

To investigate the effect of error in velocity information on the TOFE sizing result, a systematic error was introduced into the synthetic data by increasing the wavespeed in the y-direction by 2%. Then the TOFE method was applied to the resulting synthetic data for the round ellipsoid in Table 2 using the same initial guesses as the those used previously. The sizing results are shown in Table 3. In the case of one-sided scanning(where we used the same measurement points and the transducer look-angles as those used in the case of error free synthetic data), the best-fit ellipsoid turned out to be an ellipsoid greatly expanded along both the y and z coordinates as shown in the first diagram of Figure 5. Clearly, this result is not acceptable and comes from the fact that the TOFE algorithm has a relatively large number(9) of degrees of freedom. Thus, while the expanded ellipsoid matches the data points very nicely within the aperture angle of the scanning plan, its overall shape
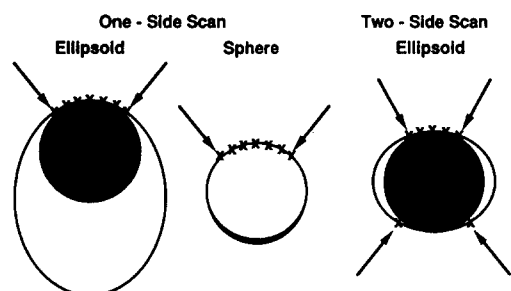
is grossly in error(Figure 5a).

One - Side Scan

Ellipsoid   **Sphere**

Two - Side Scan

Ellipsoid

Fig. 5. Schematic diagrams of the TOFE sizing results for synthetic data with a systematic error ("x" denotes the data points). actual shape : shaded figure, reconstructed shape : open figure.

Table 3. TOFE sizing results for synthetic data with systematic error.   (unit : mm)

	Two-side Scan		One-side Scan	
	Actual	(ellipsoid)	(ellipsoid)	(sphere)
X	3.0	3.0	2.9	3.0
y	5.0	5.0	4.7	5.0
z	−6.0	−6.8	−45.9	−1.9
a	20.0	19.3	28.9	
b	25.0	31.3	44.4	25.6
c	30.0	30.8	70.0	

To overcome this difficulty, two kinds of alternatives were considered. The first alternative was to keep one-sided scanning but instead fit the data to the best-fit equivalent sphere. Since the sphere has only 4 independent variables(3 centroid locations and 1 size parameter) this presumably would stabilize the algorithm. As shown in Table 3 and Figure 5b the best-fit sphere does indeed match the original round ellipsoid quite well in this particular case, Unfortunately, in the use of the best-fit sphere assumption, we lose some of the detail in the shape determination.

The second approach was to employ two-sided scanning where some of the data is taken from the "back" side of a flaw as shown in the last diagram in Figure 5. For the synthetic data set mentioned above, the two-side scanning data were simulated by simply locating the transducer at the other side

of the flaw and changing the transducer look-angle properly. Only 6 data were taken from the "back" side of the flaw with an aperture angle of 120 degrees, and 23 data were taken from the "front" side of the flaw within an aperture angle of 90 degrees. As shown in Table 3 and Figure 5c, this resulted in a best-fit ellipsoid expanded only along the y-coordinate as expected. It should be pointed out that we have found that even a single data point from the "back" side of a flaw can stabilize the TOFE method for sizing volumetric flaws. Another interesting result that we discovered with the TOFE algorithm was that for cracks, the fact that one of the dimensions of the best-fit ellipsoid is zero(and the center of the flaw is thus constrained to be in the plane of the crack) also stabilized that algorithm, like the sphere assumption, even with only one-sided scanning.

5.3 SIZING OF FLAWS IN WELDMENTS

In modern engineering applications, welded structures are very important and the accurate flaw sizing in weldments is an important element needed to improve the reliability of the structures. Thus, in this study, "flaws" in the weldments were selected ; flat-bottom holes placed in a welded specimen. Such scatterers are typically the types of deliberate "flaws" used to represent real cracks in the weldments. Figure 6 shows a schematic diagram for immersion testing of a flat-bottom hole in a welded specimen. The welded specimen was fabricated by the submerged arc welding process with the deposition of two weld passes, which completely filled the 60 degree double-V weld groove prepared on pieces of 1/2 inch(12.7 ㎜) thick mild steel plate. After the welding, the weld reinforcements were removed to get a smooth and flat specimen with a thickness of 11.5 ㎜. After this machining, 5 ㎜ diameter flat-bottom holes with a 3 ㎜ depth were fabricated both in the weldment and in the base metal.

As mentioned before, in the case of sizing flaws embedded in a specimen immersed in water, the
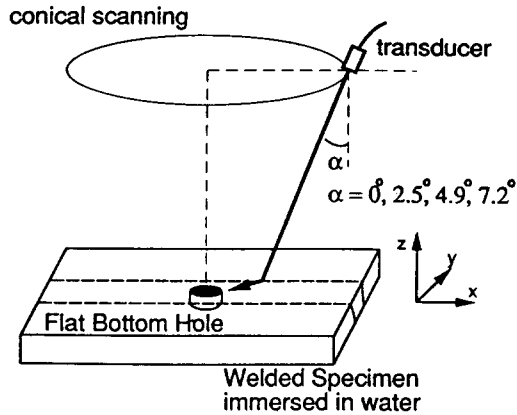
conical scanning

Fig. 6. Schematic diagram of the TOFE sizing setup for 5 ㎜ diameter flat-bottom holes fabricated in a mild steel welded specimen(immersion testing).

TOFE algorithm requires information on the location of the beam entrance point into the specimen(X_i), and the wavespeed and the propagation direction(n_z), and the time-of-flight in the specimen (refer to Figure 4). The beam entrance point(X_i) was determined by simply identifying the reflection from the front surface of the specimen. Even in the case of oblique incidence, this was able to be done because of the small tilting angle in the water. Once this incident point was calculated, the time-of-flight information required for the TOFE method could be obtained directly from the oscilloscope A-scan. Obviously, the welded joint has inhomogeneous and anisotropic material properties in general. But in the case of a mild steel welded joint, these inhomogeneities and anisotropy are not expected to be large and have been neglected. Thus, the welded specimen was treated as a homogeneous and isotropic steel plate, and its wavespeed was assumed to be constant in all directions. For each flat-bottom hole, a total of 19 data points were taken using one-sided conical scanning ; 1 data at normal incidence, and 6 at each tilting angle of $\alpha = 2.5°$, $4.9°$, $7.2°$ which corresponds to a refracted angle in the welded specimen of $10°$, $20°$, $30°$, respectively. Using these data, the TOFE scheme determined the best-fit parameters, as shown in Table 4, with only

14 and 44 iteration for the flat-bottom holes in the weldment and in the base metal, respectively, from a given set of initial guesses of the flaw centroid location($x_{cx}=0.0$, $x_{cy}=0.0$, $x_{cz}=0.0$) and the C parameters($C_{xx}=0.0$, $C_{yy}=0.0$, $C_{xx}=0.0$ $C_{xy}=0.0$, $C_{xz}=0.0$, $C_{yz}=0.0$). The final result very nicely described the major features of the bottom of the flat-bottom holes(which appear to the algorithm as flat cracks) such as the crack shape, size of the semi-axes, and orientation. The errors in the size estimates were $0.1-0.2$ ㎜ for the hole in the base metal, and $0.4-1.0$ ㎜ for the hole in the weldment. Very recently, The TOFE sizing method has also been verified experimentally for the immersion testing of composites by the author[31].

Table 4. TOFE sizing results for 5 ㎜ diameter flat-bottom holes fabricated in a mild steel welded specimen(immersion testing).
(unit : cm)

Parameter		Actual	Flat Bottom Hole	
			in Weldment	in Base Metal
location	x	0.0	0.00	0.01
	y	0.0	−0.03	0.06
	z	−0.89	−0.85	−0.87
size	a	0.25	0.21	0.24
	b	0.25	0.15	0.27
	c	0.0	0.00	0.00

6. CONCLUSIONS

In this work, we have presented some new approaches for both classifying and sizing isolated flaws inside materials using ultrasonic measurements.

In the area of flaw classification, we have demonstrated the use of probabilistic neural networks(PNN's) for the classification of welding flaws. The PNN's produced reasonable and consistent classification performances for the experimental case considered. We showed that the PNN is indeed a good choice as a classifier for these weld problems.

In the area of sizing, we have described a new time-of-flight equivalent(TOFE) sizing method for relatively large flaws in materials. We have shown

that for volumetric flaws using time-of-flight information in two sided scanning makes that algorithm stable and fast. For cracks, the method is always stable and fast, even in one-sided scanning. From our test of the TOFE method in a weldment we have shown that the method is accurate provided that the wavespeed in the material is well characterized. The excellent performance of the method observed in this study demonstrates that it can serve as a robust sizing tool for many practical applications.

In this work we have developed robust methods for both classification and sizing of flaws in materials, which can be applied to various practical applications. Extensive use has been made of a number of "tools" including digital signal processing techniques, numerical optimization algorithms and neural networks.

ACKNOWLEDGEMENTS

REFERENCES

1. International Institute of Welding, *The Evaluation of Ultrasonic Signals,* Cambridge, England : Welding Institute for International Institute of Welding, (1987).

2. International Institute of Welding, *Handbook on the Ultrasonic Examination of Welds,* Cambridge, England : Welding Institute for International Institute of Welding, (1977).

3. V. G. Shcherbinskii and V. E. Belyi : "New informative index for the nature of flaws in ultrasonic inspection," *Soviet Journal of Nondestructive Testing,* Vol. 11(1975), pp. 279－288.

4. A. K. Volpinkin : "Diffracted waves and their application in ultrasonic nondestructive testing II. Practical application of diffracted waves," *Soviet Journal of Nondestructive Testing.* Vol. 21 (1985), pp. 143－154.

5. G. J. Gruber : "Defect identification and sizing by the ultrasonic satellite-pulse technique," *Journal of Nondestructive Evaluation,* Vol. 1(1980), pp. 263－273.

6. C. P. Chiou and L. W. Schmerr : "A quasi-pulse-echo technique for ultrasonic flaw classification," *Ultrasonics,* Vol. 29(1991), pp. 471－481.

7. O. R. Gericke : "Determination of the geometry of hidden defects by ultrasonic pulse analysis testing," *Journal of Acoustical Society of America,* Vol. 35(1963), pp. 364－368.

8. O. R. Gericke : "Ultrasonic spectroscopy" in *Research Techniques in Nondestructive Testing,* Ed. R. S. Sharpe, London : Academic Press, (1970), pp. 31－61

9. D. W. Fitting and L. Adler : *Ultrasonic Spectral Analysis for Nondestructive Evaluation.* New York : Plenum Press, (1981).

10. J. L. Rose : "Element of a feature-based ultrasonic inspection system," *Materials Evaluation,* Vol. 42(1984), pp. 210－218.

11. J. L. Rose, Y. H, Jeong, and C. T. Cooper : "A methodology for reflector classification analysis in complex geometric welded structures," *Materials Evaluation,* Vol. 42(1984), pp. 98－106.

12. J. L. Rose, J. Nestleroth, L. Niklas, O. Ganglbauer, J. Ausserwoeger and F. Wallner : "Flaw classification in welded plates employing a multidimensional feature-based decision process," *Materials Evaluation,* Vol. 42, No. 4(1984), pp. 433－438, 443.

13. S. F. Burch and N. K. Bealing : "A physical approach to the automated ultrasonic characterization of buried weld defects in ferritic steel," *NDT International,* Vol. 19(1986), pp. 145－152.

14. S. F. Burch : "Objective characterization of welding defects using physical based pattern recognition techniques," in *Review of Progress in Quantitative Nondestructive Evaluation,* eds. D. O. Thompson and D. E. Chimenti, New York : Plenum Press, Vol. 7B(1988), pp. 1495－1502.

15. A. N. Mucciardi, R. Shankar and M. F. Whalen : "Application of adaptive learning networks to NDE methods," Interdisciplinary Program for

Quantitative Flaw Definition Special Report Third Year Effort, (1976).

16. M. F. Whalen and A. N. Mucciardi : "Inversion of Physically Recorded Ultrasonic Waveforms Using Adaptive Learning Network Models Trained on Theoretical Data," In *Proc. ARPA/AFML Review of Progress in Quantitative NDE.* ed. D. O. Thompson, Air Force Materials Laboratory Technical Report AFML-TR-78-205, (1979), pp. 341–367.

17. L. S. Koo : "Ultrasonic flaw classification : an approach using modelling, signal processing, and adaptive learning," Ph. D. Dissertation, Iowa State University, (1987).

18. S. M. Nugen, L. W. Schmerr, K. M. Christensen, and B. K. Lovewell : "Design and implementation of an expert system for flaw classification," *Microcomputer Application,* Vol. 9(1990), pp. 1–8.

19. L. W. Schmerr, K. E. Christensen, S. M. Nugen, L.-S. Koo and C.-P. Chiou : "Ultrasonic Flaw Classification-An Expert System Approach," in *Review of Progress in Quantitative Nondestructive Evaluation,* eds. D. O. Thompson and D. E. Chimenti, New York : Plenum Press, Vol. 8A(1989), pp. 657–664.

20. R. P. Lippmann : "An introduction to computing with neural nets," *IEEE ASSP Magazine,* April, (1987), pp. 4–22.

21. Y. H. Pao : *Adaptive Pattern Recognition and Neural Networks,* Reading : MA, Addison-Wesley Publishing Co., Inc, (1989).

22. D. E. Rumelhart, G. E. Hinton and R. J. Williams : "Learning internal representations by error propagation," in *Parallel Distributed Processing,* eds. D. E. Rumelhart, J. L. McClelland and the PDP Research Group, Cambridge, MA : MIT Press, Vol. 1(1986), pp. 318–362.

23. L. Udpa and S. S. Udpa : "Eddy current defect characterization using neural network," *Materials Evaluation,* Vol. 48(1990), pp. 342–347, 353.

24. J. M. Mann, L. W. Schmerr and J. C. Moulder : "Neural network inversion of uniform-field eddy current data," *Materials Evaluation,* Vol. 49(1991), pp. 34–39.

25. L. M. Brown and R. DeNale : "Classification of ultrasonic defect signatures using an artificial neural network," in *Review of Progress in Quantitative Nondestructive Evaluation,* eds. D. O. Thompson and D. E. Chimenti, New York : Plenum Press, Vol. 10A(1990), pp. 705–712.

26. D. Berry, L. Udpa and S. S. Udpa : "Classification of ultrasonic signals via neural networks," in *Review of Progress in Quantitative Nondestructive Evaluation,* eds. D. O. Thompson and D. E. Chimenti, New York : Plenum Press, Vol. 10A(1990), pp. 697–704.

27. D. F. Specht : "Probabilistic neural networks for classification, mapping, of associative memory," in *Proceedings of the IEEE International Conference on Neural Networks,* Vol. 1(1988), pp. 525–532.

28. D. F. Specht : "Probabilistic neural networks," *Neural Networks,* Vol. 3(1990), pp. 109–188.

29. D. F. Specht : "Probabilistic neural networks and polynomial adaline as complementary techniques for classification," *IEEE Transactions on Neural Networks,* Vol. 1, No. 1, (1990), pp. 111–121.

30. D. F. Specht : "Enhancements to probabilistic neural networks", *Proceedings of the IEEE International Joint Conference on Neural Networks,* Vol. 1(1992), pp. 761–768.

31. R. D. Thompson and D. O. Thompson : "Ultrasonics in nondestructive evaluation", *Proceedings of the IEEE,* Vol. 73(1987), pp. 176–1775.

32. R. B. Thompson : "Quantitative ultrasonic nondestructive evaluation methods", *Transactions of ASME/ Journal of Applied Mechanics,* Vol. 50(1 983), pp. 1191–1201.

33. J. Krautkramer and H. Krautkramer : *Ultrasonic Testing of Materials,* 4th Edition, New York : Springer-Verlag, (1990).

34. J. Krautkramer : "Determination of the size of defects by the ultrasonic impulse echo methods", *British Journal of Applied Physics.* Vol. 10(1959), pp. 240–245.

35. L. W. Schmerr and A. Sedov : "The flat-bottom hole : an ultrasonic scattering model", *Research in Nondestructive Evaluation,* Vol. 1(1989), pp.

181－196.

36. A. Sedov, L. W. Schmerr, and S. J. Song : "Ultrasonic scattering of a flat-bottom hole in immersion testing : an analytic model". *Journal of Acoustical Society of America*, Vol. 92(1992), pp. 578－486.

37. S. J. Song, L. W. Schmerr and A. Sedov : "DGS Diagrams and Frequency Response Curves for a flat-bottom hole : A model-based approach", *Research in Nondestructive Evaluation*, Vol. 3(1991), pp. 201－219.

38. M. G. Silk, A. M. Stoneham and J. A. G. Temple : *The Reliability of Nondestructive Inspection*, Bristol, Enland : Adam Hilger, (1987).

39. M. G. Silk : "Sizing crack-like defects by ultrasonic means", in *Research Techniques in Nondestructive Testing*, Ed. R. S. Sharpe, Ch. 2, London : Academic Press, Vol. 2(1977).

40. M. G. Silk : "The use of diffraction based time-of-flight measurements to locate and size defects", *British Journal of NDT*, Vol. 26(1984), pp. 208－213.

41. J. P. Charlesworth and J. A. G. Temple : *Engineering Applications of Ultrasonic Time-of-Flight Diffraction*, Somerset, England : Research Studies Press, (1989).

42. G. J. Gruber, G. J. Hendrix and W. R. Schick : "Characterization of flaws in piping welds using satellite pulses", *Materials Evaluation*, Vol. 42(1984), pp. 426－432.

43. C. F. Schueler, H. Lee and G. Wade : "Fundamentals of digital ultrasonic imaging", *IEEE Transactions on Sonics and Ultrasonics*, Vol. SU-31(1984), pp. 195－217.

44. J. Seydel : "Ultrasonic synthetic-aperture focusing techniques", In *Research Techniques in Nondestructive Testing*, Ed. R. S. Sharpe, New York : Academic Press, Vol, VI(1982), pp. 1－48.

45. S. O. Harrold : "Ultrasonic focusing techniques", in *Research Techniques in Nondestructive Testing*, Ed. R. S. Sharpe, New York : Academic Press, Vol. VI(1982), pp. 49－106.

46. B. Grohs, O. A. Barbian, W. Kappes, H. Paul, R. Licht and F. W. Hoh : "Characterization of flaw location, shape, and dimensions with the ALOK system", *Materials Evaluation*, Vol. 40(1 982), pp. 84－89.

47. B. P. Hildebrand and B. B. Brenden, *An Introduction to Acoustical Holography*, New York : Plenum Press, (1972).

48. L. S. Koo, H. R. Shafiee, D. K. Hsu, S. J. Wormley and D. O. Thompson : "Two-dimensional ultrasonic tomography in nondestructive evaluation by using area functions", *IEEE Transactions on Ultrasonics, Ferroelectrics, and Frequency Control*, Vol. 37(1990), pp. 148－158.

49. D. K. Hsu, J. H. Rose and D. O. Thompson : "Reconstruction of inclusions in solids using ultrasonic Born inversion", *Journal of Applied Physics*, Vol. 55(1984), pp. 162－168.

50. D. K. Hsu, D. O. Thompson and S. J. Wormley : "Reliability of reconstruction of arbitrarily oriented flaws using multiview transducers", *IEEE Transactions of Ultrasonics, Ferroelectrics, and Frequency Control*, Vol. UFFC-34(1987), pp. 508－514.

51. A. Sedov and L. W. Schmerr : "The time domain elastodynamic Kirchhoff approximation for cracks : the inverse problem", *Wave Motion*, Vol. 8(1986), pp. 15－26.

52. L. W. Schmerr, A. Sedov and C. P. Chiou : "A unified constrained inversion model for ultrasonic flaw sizing", *Research in Nondestructive Evaluation*, Vol. 1(1989), pp. 77－97.

53. L. J. Bond, C. A. Chaloner, S. J. Wormley, S. P. Neal, and J. H. Rose : "Recent advances in Born Inversion(weak scatterers)", in *Review of Progress in Quantitative Nondestructive Evaluation*, Eds. D. O. Thompson and D. E. Chimenti, New York : Plenum Press, Vol. 7A(1988), pp. 437－444.

54. C. A. Chaloner and L. J. Bond : "Investigation of the 1-D inverse Born technique", *IEE Proceedings*, Vol. 134(1987), Pt. A, pp. 257－265.

55. R. B. Thompson : "Status of implementation of the inverse Born sizing algorithm", in *Review of Progress in Quantitative Nondestructive Evaluation*, Eds. D. O. Thompson and D. E. Chimenti,

New York : Plenum Press, Vol. 4A(1985), pp. 611—621.

56. J. Yang and L. J. Bond : "Errors in determining the flaw centroid by using area functions", in *Review of Progress in Quantitative Nondestructive Evaluation*, Eds. D. O. Thompson and D. E. Chimenti, New York : Plenum Press, Vol. 11(1992).

57. C. P. Chious and L. W. Schmerr : "New approaches to model-based ultrasonic flaw sizing", *Journal of Acoustical Society of America*, Vol. 92, No. 1(1992), pp. 435—444.

58. S. J. Song and L. W. Schmerr : "Ultrasonic flaw classification in weldments using probabilistic neural networks", *Journal of Nondestructive Evaluation*, Vol. 11, No. 2(1992), pp. 69—77.

59. S. J. Song : "An ultrasonic pattern recognition approach to welding defect classification", *Journal of the Korean Society for Nondestructive Testing*, Vol. 15, No. 2(1995), pp. 395—406.

60. S. J. Song and L. W. Schmerr : "An ultrasonic time-of-flight equivalent flaw sizing method", *Research in Nondestructive Evaluation*, Vol. 4(1992), pp. 1—18.